Bubble Rise Velocity and Drag Co-efficient at High Reynolds Number in Power-Law Fluids

***HASSAN, N. M. S., KHAN, M. M. K. AND RASUL, M. G.**

College of Engineering and Built Environment
Faculty of Sciences, Engineering and Health
Central Queensland University
Rockhampton, Qld-4702
AUSTRALIA

Abstract: - Air bubbles are used in chemical, biochemical, environmental, and food process for improving the heat and mass transfer. Due to the dominance of non-Newtonian liquids used in various process industries, an understanding of bubble rise in rheologically complex liquids has grown to be important. An experimental study of the bubble rise velocity and drag co-efficient at high Reynolds number in non-Newtonian (Power-Law) fluids are presented in this paper. The main characteristics, namely, the bubble velocity and the drag relationship are investigated at high Reynolds numbers (Re<4000). The experiments were conducted in 125 mm and 400 mm cylindrical column at liquid heights of 1 m, 1.2 m, 1.4 m and 1.6 m by introducing different bubble volumes (from 0.1mL to 20.0mL) corresponding to each height. The bubble rise velocity and bubble size were measured using a combination of non-intrusive (high speed photographic) method and digital image processing. The parameters that significantly affect the rise of air bubble are identified. The effect of different liquid heights and bubble volumes on the bubble rise velocity is analysed and the influence of two different sizes of tubes on the bubble velocity for various bubble volume is discussed. A correlation of the drag coefficient at high Reynolds number is explained and compared with the results of other analytical and experimental studies available in the literature.

Key-words: - Bubble rise velocity, bubble volume, drags co-efficient, Reynolds number, power-law fluid, non-intrusive method

1 Introduction

A gas needs to be in contact with a liquid phase in any process where the gas phase is present in the form of bubbles. The bubbles find uses in many applications such as in the sparkling beverages, in the cooking processes, in the transfer of heat and mass, in the pipeline transport applications, in polymer processing and activated sludge processes and others [1].

The most significant dynamic behaviour of air bubbles are the bubble rise velocity, trajectory and the drag coefficient. The drag coefficient correlates the drag force exerted on a moving air bubble to its terminal velocity and projected surface area. The terminal velocity of an air bubble is termed as the velocity attained at steady state conditions where all applied forces are balanced. The bubble rise velocity and drag coefficient of an air bubble are mainly depended on the liquid and the properties of the bubble. In small-Reynolds numbers flows, the viscous forces are large relative to internal terms and the viscous shear stresses transmit the motion of the bubble far into the flow. So the viscosity forces dominate the terminal motion and terminal rise velocity increases with diameter of the bubble at very low Reynolds number. An intermediate region (Re>1), bubbles are no more spherical as their size increased and terminal velocity may increase or remain constant or decrease with equivalent diameter of the bubble. In this region, surface tension and inertia forces determine the terminal rise velocity. On the other hand, in very high Reynolds number flow the viscous shear stresses only affect the flow close to the wall so a thin boundary layer forms near the bubble where the velocity varies from the (relative velocity between the bubble and medium) value to approximately zero. The flow outside of this layer is caused by the pressure gradients. The adverse pressure gradient formed as the flow moves around the back of the bubble causes the flow to separate from the bubble. The location of this flow separation and the nature of the separation (either steady or unsteady) are calculated by the interaction between the pressure gradients outside the boundary layer and the viscous flow near the bubble so it is determined by the Reynolds number of the flow. At high Reynolds number, bubbles are spherical cap or mushroom shaped and the motion of the bubble is dominated by the inertia forces. In this region, bubble rise velocity increases with the equivalent diameter of the bubble [15].

A bubble rise characteristic in Newtonian liquid has received considerable attention and is well understood. Due to the dominance of non-Newtonian liquids used in various process industries, an understanding of bubble rise in rheologically complex liquids has grown to be important. The dynamic of the bubble characteristics in a gas-liquid system are still not totally understood. Many researchers have undertaken various studies to predict the actual phenomena of the bubble rise in a column of non-Newtonian liquid since last century [1-16]. The relationship between the terminal velocity and volume for larger gas bubbles were investigated by Dewsbury et al. in non-Newtonian power-law fluids [3]. Margaritis et al. studied the drag co-efficient variation for bubbles over a wide range of Re in different non-Newtonian polysaccharide solutions and proposed a correlation which matched very well with experimental data [2]. A new drag correlation for rising spheres in power-law liquids was presented by Dewsbury et al. which is valid for $0.1<Re<25000$ and described the relationship between C_d and Re in creeping, transitional, turbulent and even critical flow regimes[4]. For the case of power-law non-Newtonian fluids, it has been shown that the drag curve for air bubbles followed Hadamard-Rybczynski model rather than Stokes model for $Re < 5$ [5, 6]. But on the other hand, Miyahara and Yamanaka reported for the case of highly viscous non-Newtonian liquid that the drag coefficient deviated from the Hadamard –Rybczynski type equation if the Reynolds number increased [6]. Dhole et al. investigated that the drag co-efficient always increased with the increase in power law index for all values of the Reynolds number [7].

There have been limited studies available in the literature on bubble rise velocity and drag co-efficient of spherical and non-spherical bubble at high Reynolds numbers in non-Newtonian power-law fluids. More research and in–depth analysis on bubble rise phenomena in non-Newtonian fluid is necessary as most of the industrial fluids are non-Newtonian in nature. The aim of this study is to investigate the behaviour of the bubble rise velocity and drag co-efficient of spherical and non-spherical bubble in non-Newtonian power liquids. The correlation of drag co-efficient of the bubble at high Reynolds number is compared with the results of other analytical and experimental studies available in the literature.

2 Experimental and Calculation

The experimental set up selected in this study was similar to that used by Dewsbury et al. [3]. The experimental apparatus is shown schematically in Fig. 1. Two-test rigs were used for investigating the bubble rise characteristics in xanthan gum and polyacrylamide solution. The first rig consisted of a polycarbonate tube approximately 1.8 m in height and 125 mm in diameter. The bubble insertion mechanism consisted of a ladle or spoon that had a capability to control the injection of air. The second rig was designed with acrylic tube of 400 mm in diameter and 2.0 m in height. Larger sizes of bubble were tested in this rig to eliminate the wall effect. The camera lifting apparatus stands approximately 2.0 m high which allows the movement of the camera mount device to move through roughly 1.8 m in height. The variable speed drive of camera lifting apparatus regulates the control of the camera mount device. This drive allows the camera to be raised at approximately the same velocity as the bubble. A high speed digital video camera (Panasonic, NV-GS11, 24X optical Zoom, made in Japan) was mounted on a camera mount device with a small attachment to the side of the camera lifting apparatus.

Bubble rise velocities were computed by a frame by frame analysis of successive images. The bubble images were analysed with the software "Windows Movie Maker" by which the bubble rise time was recorded and velocity was measured. Bubble equivalent diameter was measured from the still frames which were obtained from the video image. The still images were then opened using "SigmaScan Pro 5.0" commercial software and the bubble height (d_h) and the bubble width (d_w) were measured in pixels. The pixel measurements would then be converted to millimetres based on calibration data for the camera. The bubble equivalent diameter, d_{eq} was determined [10] as

$$d_{eq} = \left(d_h \times d_w^{\,2}\right)^{\frac{1}{3}} \qquad (1)$$

where d_w the long axis length and d_h is the short axis length of the bubble. For this measurement it was assumed that the bubble was axi-symmetric with respect to its short axis direction.

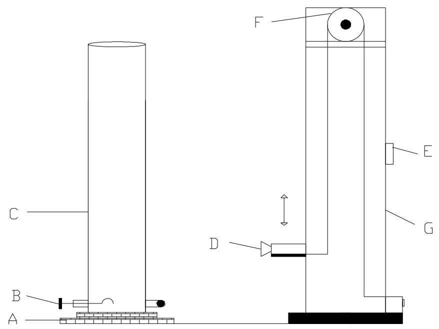

Fig. 1 Schematic diagram of experimental apparatus
A = Sturdy Base; B = Rotating Spoon; C = Cylindrical test rig (0.125m or 0.40 m diameter), D = Video camera; E = Variable speed motor; F = Pulley; and G = Camera lifting apparatus.

Since the fluid viscosity varies as a function of the shear rate so the terminal velocity of the bubble also changes with the change in shear rate. The average shear rate over the entire bubble surface is equal to U_b/d_b so the apparent viscosity can be written [2, 9] as

$$\mu = K\left(U_b/d_b\right)^{n-1} \quad (2)$$

In the case of spherical bubble, the Reynolds number for non-Newtonian power law fluid was defined as

$$\mathrm{Re} = \frac{\rho_{liq} d_b^n U_b^{2-n}}{K} \quad (3)$$

For a non-spherical bubble with a vertical axis of symmetry, the Reynolds number was defined [2, 3, 9, 11] by

$$\mathrm{Re} = \frac{d_w^n U_b^{2-n} \rho_{liq}}{K} \quad (4)$$

The drag co-efficient for spherical bubble was calculated by

$$C_d = \frac{4 g d_b \Delta\rho}{3\rho_{liq} U_b^2} \quad (5)$$

In the case of non-spherical bubble, the drag co-efficient was computed by

$$C_d = \frac{4 g d_{eq}^3 \Delta\rho}{3\rho_{liq} d_w^2 U_b^2} \quad (6)$$

The drag co-efficient for non-spherical bubble was calculated on the basis of the real bubble geometry in equation (6), where d_{eq} is the equivalent sphere diameter and d_w is the diameter of the horizontal projection of bubble or long axis length of the bubble.

3 Material Used

The xanthan gum and polyacrylamide solutions used in this study were a non-Newtonian (shear thinning pseudoplastic) fluid type. The solutions (polyacrylamide and xanthan gum) with concentration of 0.025% (by weight) were used. The temperature of all solutions in this study was maintained at $25^\circ C$. For every solution, the measured density of the solution was very close to the density of water at $25^\circ C$ since they were low concentration liquids. Rheological properties of the solutions were measured using an ARES (Advanced Rheometric Expansion System) rheometer. The rheological properties for different solutions are summarized in Table 1. The usual range of shear rates to determine fluid rheology was 1 -650s^{-1}.

Table 1 Rheological and physical properties of polymer solutions

Fluid Type	Concentration (%)	K, $Pa.s^n$	n	Density, kg/m^3
Polyacrylamide	0.025	0.00502	0.8544	998.0
Xanthan Gum	0.025	0.00720	0.7975	999.02

4 Results and Discussion

4.1 Bubble rise velocity

The velocity profile of xanthan gum and polyacrylamide solutions for various bubble volumes (0.1mL- 5.0mL) at different liquid heights is illustrated in Fig. 2. The Fig. 2 shows that the bubble velocity increases with the increase in bubble volume for all liquids. The average bubble velocity is observed (0.22 m/sec-0.30 m/sec) at 1.0 m height for a bubble volume up to 5mL. The velocity profile of xanthan gum and polyacrylamide solutions for various bubble volumes (0.1mL- 20mL) at different liquid heights is illustrated in Fig. 3. The Fig. 3 shows that the bubble velocity increases with the increase in bubble volume for all liquids. The average bubble velocity is observed (0.22 m/sec-0.41 m/sec) at 1.0 m height for a volume up to 20mL. The bubble velocity of xanthan gum is found slightly lower in comparison with polyacrylamide solution corresponds to the larger bubble volume of 20mL at 1.0 m height.

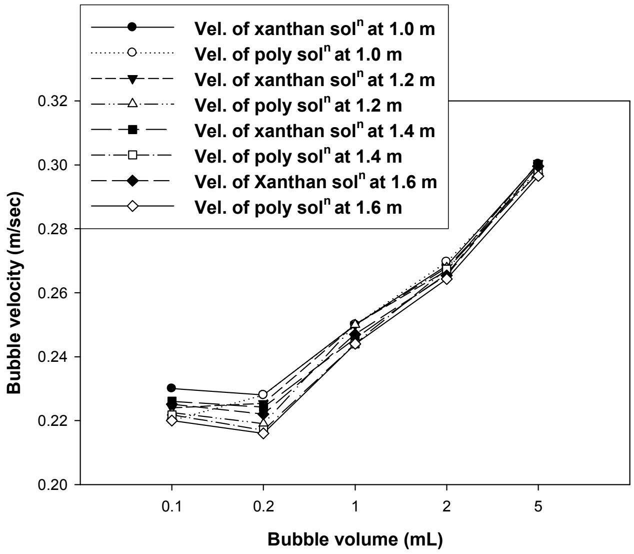

Fig. 2 Velocity profile for polyacrylamide and xanthan gum solutions at different heights (small rig)

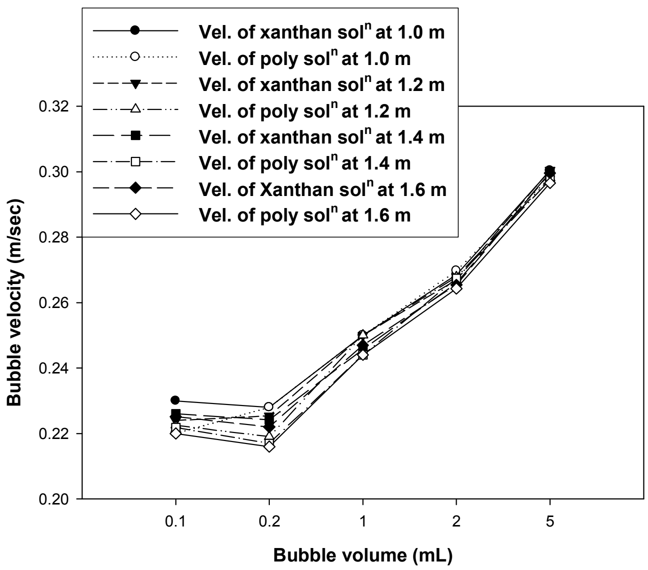

Fig. 3 Velocity profile for polyacrylamide and xanthan gum solutions at different heights (Large rig).

It can be observed from Fig. 2 and Fig. 3 that the average bubble velocity slightly decreases with the increase in liquid height but it is not significant, though the pressure changes with the increase in height is very small.

Fig. 4 presents the data obtained from both test rigs for a liquid column of 1.0 m height. It can be seen from Fig. 4 that the bubble velocity data fall on the same straight line for corresponding bubble volume and liquid height. The similar trend can also be found for all liquid heights. Hence it can be said that the bubble velocity is not dependant on rig size.

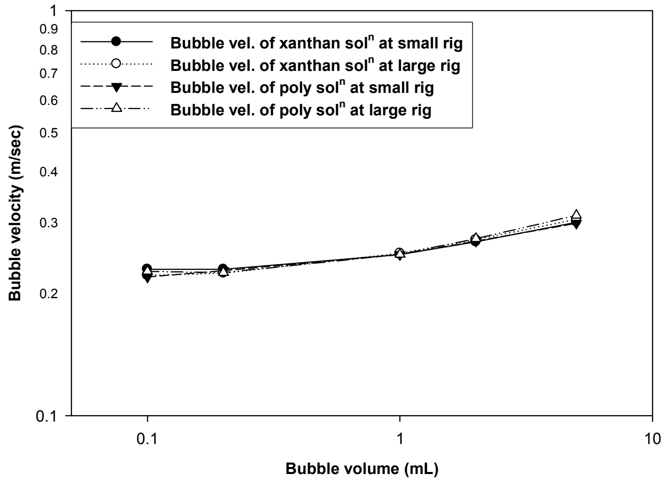

Fig. 4 Velocity profile at different rig size corresponds to the same bubble volume.

4.2 Drag co-efficient

Bubble drag coefficients as a function of Reynolds number for xanthan gum and polyacrylamide solutions are presented in Fig. 5 and Fig. 6 respectively.

No universal drag curve has been developed yet for the case of rising air bubbles in non-Newtonian power-law fluids. For $\mathrm{Re} \le 0.1$, the creeping flow regime, the governing equations can be solved to yield [12]

$$F_d = 3\pi\mu d_b U_b \tag{7}$$

which is a form of Stokes Law. This Stokes model is given by

$$C_d = \frac{24}{\mathrm{Re}} \tag{8}$$

The equation (8) is only valid for solid bubble or particle at very low Reynolds number but not suitable for gas bubbles rising in power-law liquids. The gas bubbles obey the Hadamard-Ryczynski model at very low Reynolds number which is given [6] by

$$C_d = \frac{16}{\mathrm{Re}} \tag{9}$$

As expected, models (8) and (9) fail in high Reynolds number when the current experimental data was compared.

The drag coefficient for solid particles can be determined [14] by,

$$C_d = \frac{24}{\mathrm{Re}}\left(1 + 0.173\,\mathrm{Re}^{0.657}\right) + \frac{0.413}{1 + 16{,}300\,\mathrm{Re}^{-1.09}} \tag{10}$$

The above correlation converges to Stokes model at low Re number. A modified correlation was proposed for gas bubbles in non-Newtonian power-law fluids [3], given by

$$C_d = \frac{16}{\mathrm{Re}}\left(1+0.173\,\mathrm{Re}^{0.657}\right)+\frac{0.413}{1+16{,}300\,\mathrm{Re}^{-1.09}} \quad (11)$$

The equation (11) converges to the Hadamard - Rybczynski equation, at low Reynolds number.

The following two equations (12) and (13) have been listed for spherical bubbles [13],

$$C_d = 0.28+\frac{6}{\mathrm{Re}^{0.5}}+\frac{21}{\mathrm{Re}} \quad (12)$$

$$C_d = 0.2924\left(1+9.06\,\mathrm{Re}^{-0.5}\right)^2 \quad (13)$$

The above equations are valid for (0.1< Re< 4000) and (Re < 6000) respectively. Again, the equation (12) was also used by other researcher for spherical bubble [16].
It can be seen from Fig. 5 that the deviation of the experimental C_d was initially higher in comparison with the equations (10), (11), (12) and (13) but this deviation appeared to be less with the increase in Re. For Re = 3200 and higher, it is seen that the values of the experimental C_d and the predicted C_d from these equations are nearly constant. This phenomenon is also observed in Fig.6 for polyacrylamide solution at Re= 4000 and higher.

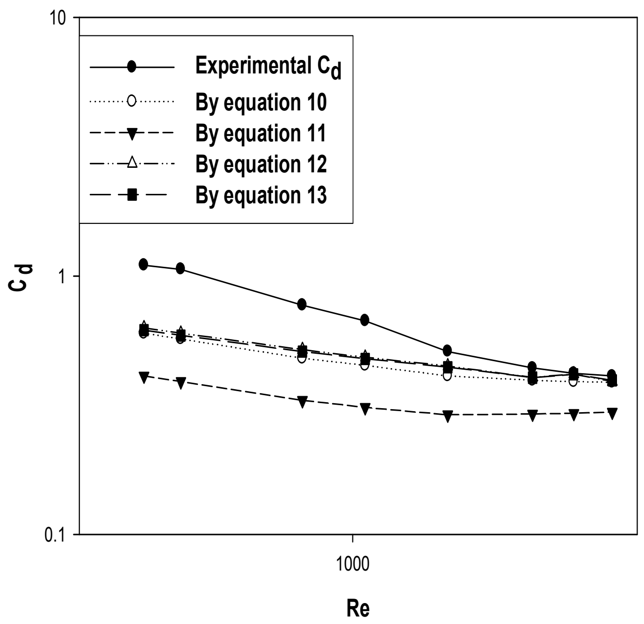

Fig. 5 Drag coefficients vs. Reynolds number for rising air bubble in xanthan gum solution.

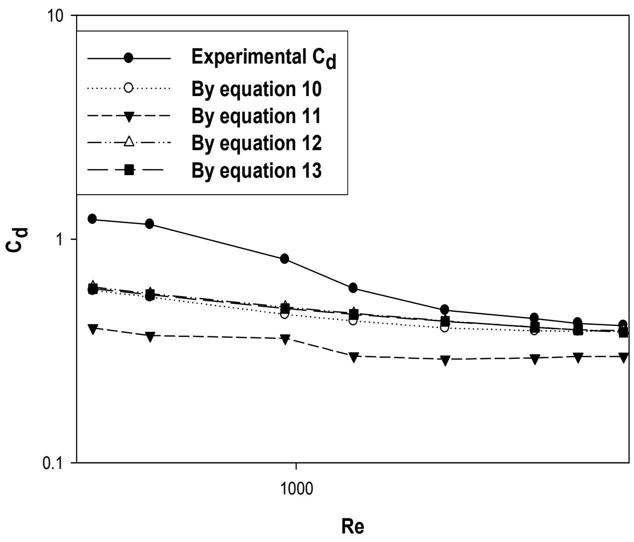

Fig. 6 Drag coefficients vs. Reynolds number for rising air bubble in polyacrylamide solution

5 Conclusions

The following conclusions can be reached from this study:

- The average bubble rise velocity increases with the increase in bubble volume for xanthan gum and polyacrylamide solutions.
- The average bubble velocity slightly decreases with the increase in liquid height for corresponding bubble volume.
- The bubble velocity of xanthan gum is found slightly lower than the velocity in polyacrylamide solution for corresponding bubble sizes.
- The bubble velocity was not dependant on the size of the test rig.
- The relationship between C_d-Re for non-Newtonian power-law fluids showed acceptable results with the available analytical and experimental studies of the literature but it deserves further study for a wide range of Reynolds number.

Nomenclature:

d_b	[m]	bubble diameter
d_h	[m]	bubble height
d_w	[m]	projected diameter onto horizontal plane

d_{eq}	[m]	equivalent sphere diameter
μ	[Pa.s]	apparent viscosity
Re	[-]	Reynolds number
C_d	[-]	drag coefficient
F_d	[N]	drag force
g	[m/s^2]	acceleration due to gravity
U_b	[m/s]	bubble rise velocity
n	[-]	power law index
K	[Pa.s^n/m^2]	consistency index

Greek letters

$\Delta\rho$	[kg/m^3]	density difference between liquid and air bubble
ρ_{liq}	[kg/m^3]	liquid density

References:

[1] Shosho, C. and Ryan, Micheal, E., An experimental study of the motion of long bubbles in inclined tubes, Chemical engineering science, 56, 2001, 2191-2204.

[2] Margaritis A., te Bokkel, D. W. and Karamanev, D. G., Bubble Rise Velocities and Drag Coefficients in non-Newtonian Polysaccharide solutions, John Wiley & Sons, Inc., 1999.

[3] Dewsbury, K., Karamanev, D. G. and Margaritis, A., Hydrodynamic Characteristics of free Rise of Light solid Particles and Gas Bubbles in Non-Newtonian Liquids., Chemical engineering Science, vol. 54, 1999, pp.4825-4830.

[4] Dewsbury, K., Karamanev, D. G. and Margaritis, A., Rising solid sphere hydrodynamics at high Reynolds numbers in non-Newtonian fluids, Chemical Engineering Journal, 87, 2002, 129-133.

[5] Dewsbury, K., Karamanev, D .G. and Margaritis, A., Dynamic Behavior of Freely Rising Buoyant Solid Spheres in Non-Newtonian Liquids, AIChE Journal, Vol. 46, No. 1, 2000.

[6] Miyahara, T. and Yamanaka, S., Mechanics of Motion and Deformation of a single Bubble Rising through Quiescent Highly Viscous Newtonian and non-Newtonian Media, Journal of chemical engineering, Japan, Vol. 26, No. 3,1993.

[7] Dhole, S. D., Chhabra, R. P. and Eswaran, V., Drag of a Spherical Bubble Rising in Power Law Fluids at Intermediate Reynolds Numbers., Ind. Eng. Chem. Res. 46, 2000, 939 – 946.

[8] Zheng, Li and Yapa, P. D., Buoyant Velocity of Spherical and Non spherical Bubbles/Droplets, Journal of Hydraulic Engineering, Vol. 126, No.1 , 2000.

[9] Lali, A. M., Khare, A. S., Joshi, J. B. and Nigam, K. D. P., Behaviour of Solid Particles in viscous Non-Newtonian Solutions: Settling Velocity, Wall Effects and Bed Expansion in Solid-Liquid Fluidized Beds, Powder Technology, 57, 1989, 39 – 50.

[10] Lima-Ochoterena, R. and Zenit, Visualization of the flow around a bubble moving in a low viscosity liquid, Revista Mexicana De Fisica 49 (4), 2003, 348 – 352.

[11] Miyhara, T. and Takahashi, T., Drag coefficient of a single bubble rising through a quiescent liquid., International Chemical Engineering, Vol. 25, No. 1, 1985.

[12] Chhabra, R. P., Bubbles, Drops, and Particles in Non-Newtonian Fluids, Taylor & Francis Group CRC Press, 2006.

[13] Clift, R., Grace, J. R and Weber, M. E., Bubbles, Drops and Particles; Academic Press, 1978, republished by Dover, 2005.

[14] Turton, R., and Levenspiel, O., A short note on the drag correlation for spheres, Powder Technology, 4, 1986.

[15] Kulkarni, A. A. and Joshi, J. B., Bubble Formation and Bubble Rise Velocity in Gas-Liquid Systems: A Review, Ind. Eng. Chem. Res., 44, 2005, 5873-5931.

[16] Zhang, Y. and Reese, J. M., The drag force in two-fluid models of gas–solid flows, chemical Engineering Science 58, 2003, 1641-1644.